International Journal of Fluid Power 9 (2008) No. 3 pp. 7-18

EQUIVALENT TIME-INVARIANT MODELLING OF ELECTROHYDRAULIC ACTUATORS WITH APPLICATION TO ROBUST CONTROL SYNTHESIS

Mark Karpenko and Nariman Sepehri*

Fluid Power Research Laboratory, Department of Mechanical and Manufacturing Engineering,
University of Manitoba, Winnipeg, Manitoba, R3T 5V6
**corresponding author; email: nariman@cc.umanitoba.ca*

Abstract

An important aspect of robust control development around hydraulic actuators is establishing a set of equivalent linear time-invariant (LTI) models that describe the dynamics of the system over the desired envelope of operation. The nonlinearities inherent in the hydraulic functions must be recast into an equivalent linear form in order to make the robust control problem amenable to solution by linear techniques. This paper develops a simple model-based approach for evaluating equivalent LTI frequency response functions of an electrohydraulic actuator by Fourier transformation of acceptable actuator input-output data. The efficacy of the numerical procedure is compared with two other available methods, namely small-signal analysis and Golubev's least-squares approach. It is shown that the proposed approach can describe large signal effects and at the same time properly characterize the features of the hydraulic actuator frequency response that are important for robust control design, without the need for *a priori* information about the asymptotic behaviour or structure of the equivalent LTI transfer function. The applicability of the proposed numerical technique towards development of practical controllers for fluid power systems is demonstrated by the results of a typical robust control design example for an experimental electrohydraulic positioning system.

Keywords: electrohydraulic actuators, robust control synthesis, equivalent linear time-invariant modelling, frequency response functions, Fourier transformation

1 Introduction

Despite widespread use of fluid power devices, control system development for hydraulic actuators remains a challenging task. The main issue that must be overcome is the nonlinear behaviour of the system functions, for example the nonlinear relationship between pressure and flow in the servovalve. Other difficulties include coping with uncertainty in the hydraulic system parameters, whose values can vary with operating conditions or as a result of faults. To overcome these challenges, a number of different approaches have been applied for development of fluid power control systems, including state feedback (Finney et al, 1985), adaptive control (Plummer and Vaughan, 1996), Lyapunov based control (Sekhavat et al, 2005), and soft computing (Kim and Lee, 2006). Robust control techniques such as H_∞ and quantitative feedback theory (QFT), have also received a good deal of attention in the fluid power literature (Piche et al., 1991; Karpenko and Sepehri, 2003; Niksefat et al., 2007).

This manuscript was received on 27 April 2008 and was accepted after revision for publication on 8 August 2008

One feature that makes robust control techniques appealing for control system design around hydraulic actuators is the possibility of desensitizing the control loop to plant nonlinearities and parameter variations using a fixed-gain control structure. This is in contrast to other approaches, such as adaptive control, which deal with system nonlinearities in an on-line fashion. Moreover, with robust control techniques, good transient and steady-state performance can often be obtained using only the controlled variable as feedback. This is attractive from the perspective of industrial implementation (Niksefat et al., 2007). However, most robust control theories, including QFT, are based on the assumption that the system to be controlled is a linear one. Therefore, a key element in the application of robust synthesis techniques for control of hydraulic actuators is the necessity to express the nonlinear dynamics as a set of equivalent linear time-invariant (LTI) functions.

An equivalent LTI function is one that generates the same output as the nonlinear system when driven by

the same input signal. A set of equivalent LTI functions is required to deal with parametric uncertainty in the original nonlinear plant and to handle the fact that the plant output is dependent upon the strength of the input. One of the most simple and common approaches for translating the nonlinear hydraulic actuator dynamics into an equivalent LTI form is to linearize the hydraulic functions around a steady-state operating point (Merritt, 1967). The development of linearized models is an effective way to gain insight into how the dynamics of systems and components interact (Wu et al., 2002). However, with this method, it is only possible to approximate the system dynamics by a linear plant over a limited region of operation. Since small-signal assumptions can be violated during the operation of the system, great care must be exercised in the use of linearized analysis for controller design (Edge, 1997). Part of the objective of this paper is to demonstrate that fixed parameter linearized models are indeed inadequate to describe the hydraulic system transient response.

An alternative approach for establishing an equivalent LTI representation of hydraulic actuators is to employ the concept of restricted device equivalence (Horowitz, 1993), where the equivalent LTI function is found by evaluating the transforms of the actuator input-output signals and taking their ratio in the frequency domain. This is also called the *LTI-equivalent* (LTIE) approach (Horowitz, 1981). An important difference between small-signal and LTIE transfer functions is that LTIE functions are not subject to small-signal assumptions and can properly characterize large signal responses using a fixed-gain structure, a requirement demanded by most robust synthesis theories. An additional advantage associated with LTIE modelling is that Schauder's fixed point theorem can be applied to prove that the compensator which solves the equivalent LTI problem also solves the original nonlinear control problem (Horowitz, 1993).

The first step to derive LTIE functions for a hydraulic actuator is to obtain a set of acceptable input-output responses from a model of the nonlinear system. Then, a model identification technique must be used to translate the time-domain data into the frequency domain for controller synthesis. The only paper that employs the LTIE approach for fluid power systems is the work of Niksefat and Sepehri (2007), which developed a numerical approach for inverting the hydraulic actuator dynamics and used Golubev's least-squares method (Golubev and Horowitz, 1982) for identifying the LTIE transfer functions of an experimental hydraulic actuator. In Niksefat and Sepehri (2007), only low-order models of the hydraulic system were identified. It was also observed that Golubev's algorithm could improperly characterize the inherent integration characteristic of the ram. Therefore, more attention must be directed towards establishing suitable techniques for identification of LTIE hydraulic actuator models from time-domain data.

This paper develops a simple numerical procedure for constructing hydraulic actuator LTIE frequency response functions directly from the actuator input-output pairs. The LTIE frequency response functions provide all the information required for robust synthesis and are obtained by numerical integration of the continuous time Fourier integral. Therefore, the frequency response functions can be obtained without the need for *a priori* knowledge about the asymptotic behaviour or structure of the LTIE transfer function as is required by other identification approaches, such as Golubev's method. Additionally, the proposed numerical approach employs an extra term that improves accuracy as compared to the conventional discrete Fourier transform, which is typically applied to evaluate Fourier integrals. Further, it is demonstrated that the presented technique can accurately characterize the hydraulic actuator magnitude and phase response over a wide range of frequencies and properly capture large signal effects.

The applicability of the proposed numerical technique towards development of a practical controller for a hydraulic actuator is demonstrated by the results of a robust control design example. Quantitative feedback theory is used to design a low-order position controller for an experimental hydraulic ram that gives good transient and steady-state performance over a wide range of parameter uncertainty and without the need for additional tuning. It is also shown that the LTIE approach enables the synthesis of a near optimal control law, in terms of minimizing feedback.

2 System Under Investigation

The electrohydraulic system under investigation is shown in Fig. 1. The ram is a double rod type, operated under position control against a spring-force dominant load. The nonlinear state equations that describe the relationship between the servovalve control flows, Q_1 and Q_2, and the actuator position output, x_p, are (Karpenko and Sepehri, 2003):

$$\dot{x}_p = v_p \tag{1a}$$

$$\dot{v}_p = \frac{1}{m}\left(AP_1 - AP_2 - dv_p - kx_p\right) \tag{1b}$$

$$\dot{P}_1 = \frac{\beta_h}{V_1}\left(Q_1 - Av_p\right) \tag{1c}$$

$$\dot{P}_2 = \frac{\beta_h}{V_2}\left(-Q_2 + Av_p\right) \tag{1d}$$

In Eq. 1, m, d, A, and β_h are the mass of the piston, the effective viscous damping of the actuator, the piston annulus area, and the bulk modulus of the hydraulic fluid, respectively. Pressures P_1 and P_2 denote the hydraulic pressures in each of the two actuator chambers, and k refers to the stiffness of the load. The volume of hydraulic oil on each side of the piston is given by variables V_1 and V_2.

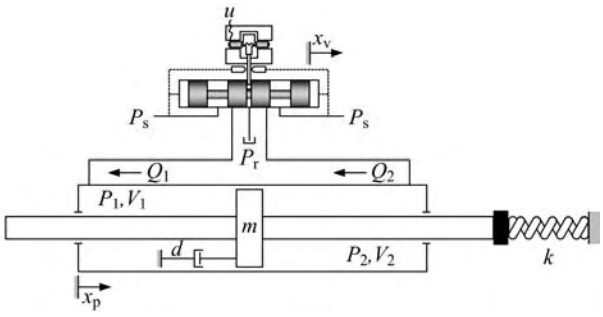

Fig. 1: ***Electrohydraulic positioning system***

The servovalve control flows are given by (Merritt, 1967)

$$Q_1 = K_v w x_v \sqrt{\frac{P_s - P_r}{2} + \frac{x_v}{|x_v|}\left(\frac{P_s + P_r}{2} - P_1\right)} \tag{2a}$$

$$Q_2 = K_v w x_v \sqrt{\frac{P_s - P_r}{2} + \frac{x_v}{|x_v|}\left(P_2 - \frac{P_s + P_r}{2}\right)} \tag{2b}$$

which are valid for both extending and retracting strokes. Pressures P_s and P_r in Eq. 2 refer to the hydraulic supply and return pressures and constants K_v and w are the flow coefficient and orifice area gradient of the servovalve. The valve flow coefficient is computed as $K_v = C_d\sqrt{2/\rho}$ where C_d is the servovalve orifice coefficient of discharge and ρ is the density of the hydraulic fluid. Variable x_v is the displacement of the servovalve spool.

Finally, the relationship between the control signal, u, and the position of the servovalve spool is modelled as a second-order lag (Karpenko and Sepehri, 2003) having undamped natural frequency ω_v, damping ratio ζ_v, and valve spool position gain, k_{sp}. Therefore, the equivalent LTI frequency response function relating the change in the position of the ram $X_p(j\omega)$ to the change in the servovalve command signal $U(j\omega)$ can be written as

$$\frac{X_p(j\omega)}{U(j\omega)} = P_V(j\omega)P_H(j\omega) \tag{3}$$

where $P_V(j\omega) = \dfrac{k_{sp}\omega_v^2}{(j\omega)^2 + 2\zeta_v\omega_v(j\omega) + \omega_v^2}$ describes the second-order servovalve spool dynamics. Function $P_H(j\omega)$ refers to the equivalent LTI frequency response that captures the nonlinear relationship between the servovalve spool displacement, x_v, and the actuator position, x_p.

To identify functions P_H, a set of acceptable input-output responses must first be obtained from nonlinear model Eq. 1. To do this, a family of acceptable output responses is defined as

$$\mathcal{X}_p^a(s) = \mathcal{R}(s)\mathcal{T}(s) \tag{4}$$

where $X_p^a(s) \in \mathcal{X}_p^a(s)$ is the acceptable position response to the reference command $R(s) \in \mathcal{R}(s)$. $\mathcal{T}(s) = \{T(s)\}$ is the set of acceptable closed-loop system functions, which map each reference input to an output response in set $\mathcal{X}_p^a(s)$. A simple description of system function $T(s)$ for a hydraulic actuator is

$$T(s) = \frac{\left(\frac{s}{\lambda}+1\right)}{\left(\frac{s}{p_1}+1\right)\left(\frac{s}{p_2}+1\right)\left(\frac{s^2}{\omega_p^2} + \frac{2\zeta_p}{\omega_p}s + 1\right)} \tag{5}$$

In Eq. 5, the locations of the transfer function poles are fixed to set the main characteristics of the actuator response. Some variation in the output of the hydraulic actuator is, however, inevitable due to system nonlinearities and parametric uncertainties. The acceptable range of variation in the closed-loop responses is regulated by adjusting parameter λ. Figure 2a shows a typical acceptable hydraulic actuator position response obtained using Eq. 5.

Once the acceptable output set has been defined, the time history of the input signal, x_v, required to drive the ram the along the acceptable closed-loop trajectory must be calculated. A suitable procedure for computing the inverse dynamics of the hydraulic actuator has been developed in Niksefat and Sepehri (2007), and is briefly outlined in the Appendix. This method was used to compute the time history of the servovalve spool displacement shown in Fig. 2b. The nominal parameter values of an existing hydraulic test rig (Karpenko and Sepehri, 2003), listed in Table 2 (see Section 5), were used to obtain the plot. Together, the time histories of the valve spool displacement and actuator position response form an input-output pair that can be used to identify the equivalent LTI model of the hydraulic actuator. Many such signal pairs are normally required for control system synthesis to ensure that the nonlinear actuator dynamics are adequately represented over the operational envelope of the system.

3 Hydraulic Actuator Frequency Response by Small-Signal Approach

Expanding Eq. 2 as a truncated Taylor series around a fixed operating point o, the linearized servovalve flows are

$$\begin{aligned} Q_1 &\approx Q_{1o} + \frac{\partial Q_1}{\partial x_v}(x_v - x_{vo}) + \frac{\partial Q_1}{\partial P_1}(P_1 - P_{1o}) \\ &\approx Q_{1o} + K_{1f}(x_v - x_{vo}) - K_{1p}(P_1 - P_{1o}) \end{aligned} \tag{6}$$

$$\begin{aligned} Q_2 &\approx Q_{2o} + \frac{\partial Q_2}{\partial x_v}(x_v - x_{vo}) + \frac{\partial Q_2}{\partial P_2}(P_2 - P_{2o}) \\ &\approx Q_{2o} + K_{2f}(x_v - x_{vo}) + K_{2p}(P_2 - P_{2o}) \end{aligned} \tag{7}$$

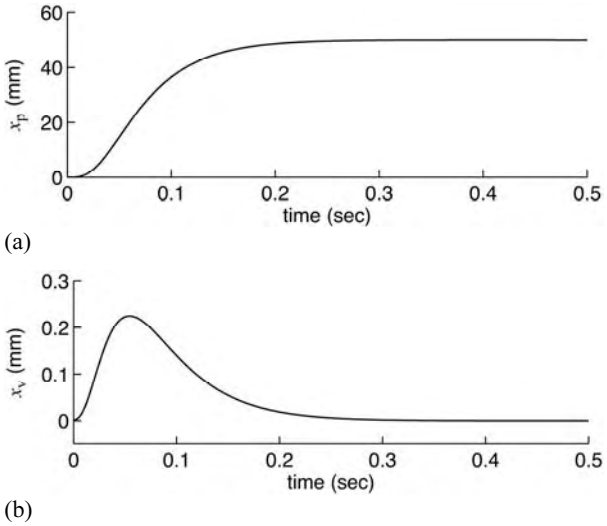

Fig. 2: *Typical acceptable hydraulic actuator input-output response obtained using (5) with P_1 = 15, p2 = 20, ωp = 852, ζp = 1, and λ = 14: (a) actuator position (output); (b) servovalve spool displacement (input)*

Partial derivatives $\frac{\partial Q}{\partial x_v}$ are known as the valve flow gains and partial derivatives $\frac{\partial Q}{\partial P}$ are called the flow-pressure coefficients. For an equal area ram driven by a matched and symmetrical valve with $P_r = 0$, the pressure in one cylinder half rises above $P_s/2$, while the pressure in the other cylinder half decreases below $P_s/2$ by roughly the same amount (Merritt, 1967). Thus, for an extending stroke, the individual cylinder pressures are $P_1 \approx \frac{1}{2}(P_s + P_L)$ and $P_2 \approx \frac{1}{2}(P_s - P_L)$, where $P_L = P_1 - P_2$ is the load pressure. Due to the relationship between P_1 and P_2, it is quite often the case that $K_{1f} \approx K_{2f}$ and $K_{1p} \approx K_{2p}$. The valve coefficients can therefore be written in terms of the operating point load pressure as follows:

$$K_f = K_v w \sqrt{\frac{1}{2}\left(P_s - \mathrm{sgn}(x_{vo}) P_{Lo}\right)} \tag{8}$$

$$K_p = \frac{K_v w x_{vo}\, \mathrm{sgn}(x_{vo})}{2\sqrt{2(P_s - \mathrm{sgn}(x_{vo}) P_{Lo})}} \tag{9}$$

Laplace transforms of Eq. 1 are now combined with Eq. 6 and Eq. 7 to derive the small-signal hydraulic actuator transfer function

$$P_H(s) = \frac{\beta_h A K_f (V_T s + 2AK_p)}{\left\{\begin{array}{c}(ms^2 + ds + k)(V_{1o}V_{2o}s^2 + \beta_h K_p V_T s + 2\beta_h^2 K_p) \\ +\beta_h A^2 V_T s^2 + 2\beta_h^2 A^2 K_p s\end{array}\right\}} \tag{10}$$

where V_T is the combined volume of both cylinder halves and parameters V_{1o} and V_{2o} refer to the cylinder volumes at operating point *o*.

To use transfer function Eq. 10 for control system synthesis, the values of the servovalve flow and flow-pressure coefficients need to be evaluated at different operating points. A method for identifying the servovalve operating point, which lends itself well to graphical interpretation, is the load locus technique (Nikiforuk and Westlund, 1965). The idea is to superimpose a plot of the hydraulic load line over a plot of the nonlinear servovalve flow curves. The load line defines the relationship between the load pressure and load flow of hydraulic oil needed to drive the mechanical load. On the load locus plot, the servovalve operating points can be identified by the intersections of the load line and the valve flow curves (Nikiforuk and Westlund, 1965).

From Eq. 1b, the time history of the load pressure required to position the actuator against the load is

$$P_L(t) = \frac{1}{A}\left(m\ddot{x}_p^a(t) + d\dot{x}_p^a(t) + kx_p^a(t)\right) \tag{11}$$

The corresponding load flow through the servovalve is given approximately by

$$\begin{aligned} Q_L(t) &= \frac{Q_1 + Q_2}{2} = \frac{1}{2\beta_h}\left(\dot{P}_1 V_1 - \dot{P}_2 V_2\right) + A\dot{x}_p^a \\ &\approx \frac{1}{2\beta_h}\left[\frac{\dot{P}_L}{2} V_1 - \left(\frac{-\dot{P}_L}{2}\right) V_2\right] + A\dot{x}_p^a \\ &\approx \frac{V_1 + V_2}{2\beta_h}\dot{P}_L(t) + A\dot{x}_p^a(t) \end{aligned} \tag{12}$$

Using Eq. 11 and Eq. 12, a plot of Q_L versus P_L can be constructed for each acceptable hydraulic actuator response under consideration. The load line pertaining to the example actuator response of Fig. 2 is shown in Fig. 3. As indicated by the arrowhead, the load line is traversed from the initial actuator state at point '*a*' to the steady-state at point '*j*'. At each location where the load line intersects the valve pressure-flow curves, the servovalve operating point can be graphically evaluated by reading off the operating point valve spool displacement, x_{vo}, and the operating point load pressure, P_{Lo}. The valve coefficients can then be solved.

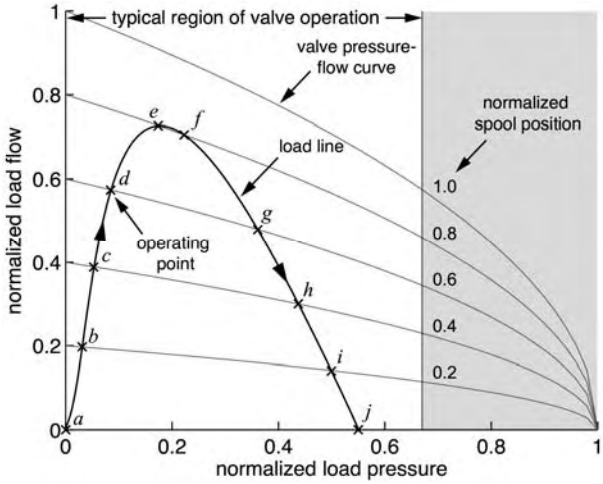

Fig. 3: *Example hydraulic load line and graphical determination of servovalve operating points for a typical actuator position response*

Table 1 reports the servovalve flow coefficients, K_f and K_p, at operating points '*a*' through '*j*'. Referring to Table 1, it is clear that the valve coefficients are

strongly time varying over the transient response interval. Figure 4 shows the responses of transfer function Eq. 10 when the values of K_f and K_p are allowed to vary over time and when the values of K_f and K_p are fixed. Although a small-signal model with time-varying parameters can accurately reproduce the transient response, such a transfer function violates the assumption of time-invariance inherent in many robust synthesis techniques. Therefore, unless the region of operation of the servovalve is suitably restricted, small-signal analysis may not be suitable for design of the robust control system.

Table 1: Servovalve coefficients pertaining to load line in Fig. 3

point	K_f (m^3/sec)	$K_p \times 10^{11}$ (m^3/Pa·sec)
a	1.78	0
b	1.75	0.28
c	1.73	0.58
d	1.70	0.90
e	1.61	1.26
f	1.57	1.30
g	1.42	1.07
h	1.33	0.77
i	1.26	0.40
j	1.19	0

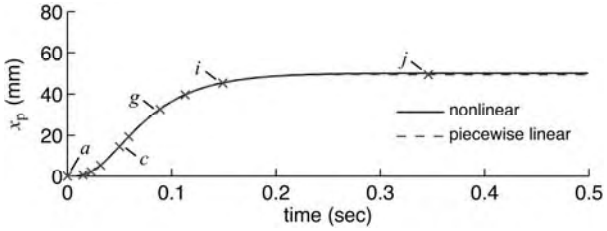

(a)

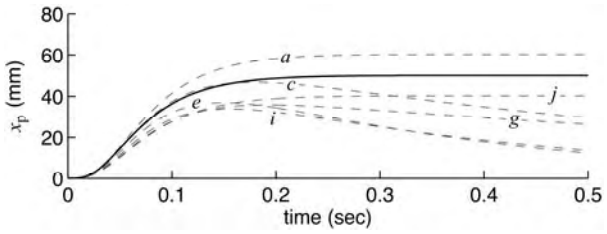

(b)

Fig. 4: *Comparison between nonlinear position response and responses of equivalent small-signal models: (a) response for time-varying Kf and Kp (marks correspond to updates of linearized valve coefficients); (b) responses for fixed values of Kf and Kp*

The Bode plots of the small-signal transfer functions at each operating point are shown in Fig. 5. It is observed that the linearization process introduces a significant amount of dynamic uncertainty in the low frequency range $\omega < 10$ rad/sec. This results from the fact that some of the small-signal models, for example the model corresponding to operating point '*f*', are type 0 because $K_p \neq 0$ during part of the system transient. However, since the servovalve meters flow, it must close when the position error is zeroed. Thus, the actuator always physically behaves as a type 1 system and the actual low frequency uncertainty is much smaller than the amount predicted by the equivalent small-signal plant set.

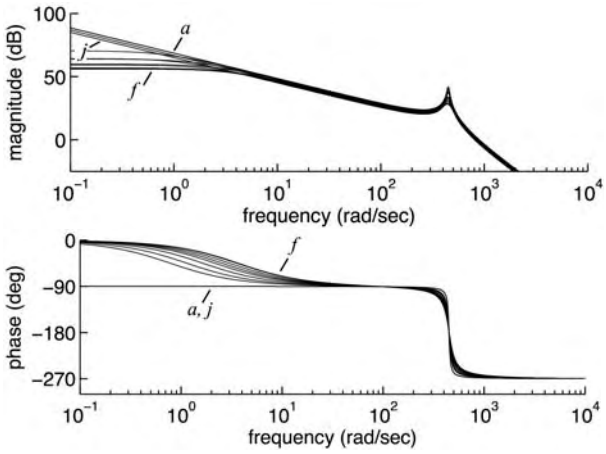

Fig. 5: *Bode plots of equivalent small-signal transfer function set pertaining to load line in Fig. 3*

Since robust control relates the amount of feedback at each frequency to the amount of uncertainty in the plant dynamics, small-signal analysis forces the magnitude of the loop transmission to be unnecessarily large in the low frequency range. The result is an over-designed and conservative control system that uses much more feedback gain than is actually required to solve the robust control problem. This point will be further elaborated on in Section 5.

4 Hydraulic Actuator Frequency Response by LTI-Equivalent Approach

4.1 Existing Approach – Golubev's Method

One approach for computing LTIE frequency response, $P_H(j\omega) = \hat{X}_p(j\omega) \big/ \hat{X}_v(j\omega)$, has been developed by Golubev and Horowitz (1982). The method allows least-squares estimates of the LTIE transfer function coefficients to be calculated by repeated integration of the plant input-output data. For the hydraulic actuator under study, the LTIE equivalent system can be described in the time domain by the following ordinary differential equation, which assumes zero initial conditions (Whitfield and Messali, 1987):

$$\begin{aligned} b_n x_p^{(n)}(t) + b_{n-1} x_p^{(n-1)}(t) + \ldots + b_0 x_p(t) \\ = a_0 x_v(t) + \ldots + a_m x_v^{(m)}(t) \end{aligned} \tag{13}$$

where $x_p^{(j)}(t) = \dfrac{d^j}{dt^j} x_p(t)$. Each side of Eq. 13 is then integrated *n*-times and rearranged to get

$$\begin{aligned} b_n x_p(t) = -b_{n-1} x_p^{(-1)}(t) - \ldots - b_0 x_p^{(-n)}(t) \\ + a_0 x_v^{(-n)}(t) + \ldots + a_m x_v^{(-n+m)}(t) \end{aligned} \tag{14}$$

The integrals in (14) are computed from samples of signals x_p and x_v taken at time instants t_k, (k = 1,2,…N). For example using the trapezoidal rule, $x_p^{(-r)}(t_k) = x_p^{(-r)}(t_{k-1}) + \frac{h}{2}\left[x_p^{(-r+1)}(t_k) + x_p^{(-r+1)}(t_{k-1})\right]$, where h is the sampling interval.

Assuming b_n=1, a least-squares problem is assembled next to solve unknown system coefficients a_i and b_j as follows

$$\left[\sum_{k=1}^{N}\phi(t_k)\phi(t_k)^T\right]\{b_0,...,b_{n-1},a_0,...a_m\}^T = \left\{\sum_{k=1}^{N}\phi(t_k)x_p(t_k)\right\} \quad (15)$$

where $\phi(t_k) = \left[-x_p^{(-n)}(t_k),...,-x_p^{(-1)}(t_k),x_v^{(-n)}(t_k),...,x_v^{(-n+m)}(t_k)\right]$. Golubev's method thus allows the LTIE transfer function to be evaluated by taking the Laplace transform of Eq. 13, and inserting the values of a_i and b_j solved from Eq. 15.

Golubev's method was applied to estimate a LTIE transfer function to fit the example hydraulic actuator input-output signal pair shown in Fig. 2. The identified transfer function is

$$P_H(s) = \frac{5.18\times10^8(s+48.6)(s+122.0)}{s(s^2+161.3s+6.8\times10^3)(s^2+8.9s+2.0\times10^5)} \quad (16)$$

The ability of the identified LTIE transfer function to reproduce the original nonlinear position response is shown in Fig. 6. As is seen, the results are indistinguishable. A Bode plot of Eq. 16 is shown in Fig. 7. It is observed that the identified LTIE transfer function properly captures two of the important features of the hydraulic actuator behaviour. The first is the inherent integration characteristic of the ram in the low frequency range, ω < 10 rad/sec. The second feature is the resonant mode in the high frequency range, ω = 500 rad/sec, that results from the interaction between the load mass and the compressibility of the hydraulic oil. Proper identification of the resonant mode is important for control system design since the resonance peaks occur when the phase lag is 180º and thus tend to limit the achievable gain margin. Another interesting characteristic of the identified LTIE transfer function is the fact that it has a more complex structure than the small-signal transfer function. The additional transfer function elements are necessary to account for large signal effects, for example dynamic changes in the values of the operating point flow coefficients, which could not be properly represented by the fixed parameter small-signal models.

In spite of the desirable features of Golubev's method, several drawbacks of the approach for hydraulic actuator model identification are noted below:

The algorithm was found by the authors to be quite sensitive to the sampling interval, h, and the length of the data record, N, used to assemble the least-squares system Eq. 15. If parameters h and N were chosen incorrectly, the algorithm was observed to generate transfer functions with unstable poles and zeros.

The length of the data record used in the approximation plays an important role in determining the frequency range over which the transfer function estimate is most accurate. Short data records had to be used to properly identify the actuator resonance, at the expense of degraded accuracy in the low-frequency range. This suggests that difficulties may be encountered when applying Golubev's method to systems having both slow and fast dynamic modes as in hydraulic actuators with internal leakage.

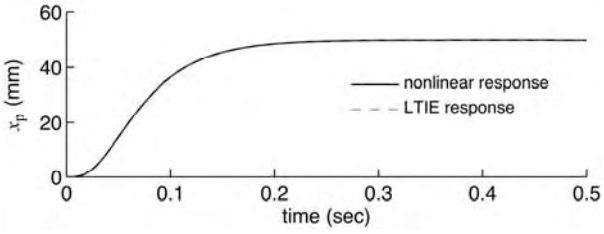

Fig. 6: *Comparison between nonlinear position response and response of LTIE transfer function obtained by Golubev's method. Results are indistinguishable*

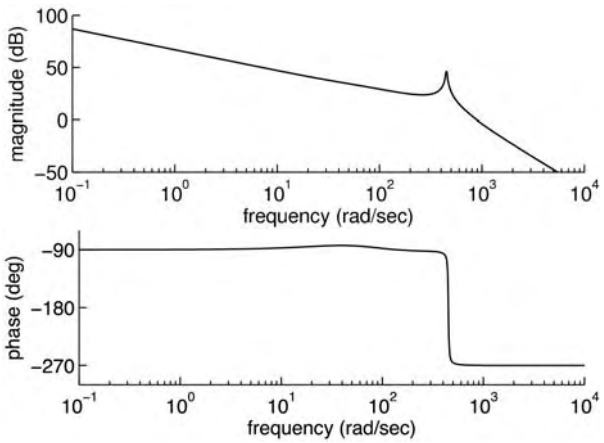

Fig. 7: *Bode plot of LTIE transfer function obtained by Golubev's method*

To obtain good transfer function fits, *a priori* information about the asymptotic behaviour of the transfer function had to be inserted into the model. For example, it was necessary to set parameter b_0 = 0 in Eq. 15 to force the LTIE transfer function to have a pole at the origin.

There is no way to decide, *a priori*, the degrees of the numerator and denominator polynomials that give the best fit of the time-domain data, even if the excess of poles over zeros is known. This makes the application of the approach tedious, if not unmanageable, in a practical design scenario where many LTIE models must be identified to represent the response of a hydraulic actuator under different operating conditions.

4.2 New Approach – Fourier Transformation

A different approach that can be used to compute LTIE frequency response $P_H(j\omega) = \hat{X}_p(j\omega)\big/\hat{X}_v(j\omega)$, which has not been applied to hydraulic actuators, is Fourier transformation. An advantage of Fourier transformation over Golubev's method is that the magni-

tudes and phase angles of the LTIE plants can be obtained directly without the need to solve a rational transfer function. The use of Fourier transformation can therefore improve the efficiency of the LTIE modelling process, the most time consuming aspect of robust control development. In this Section, a numerical procedure for evaluating the Fourier transform of the hydraulic actuator input-output signal pairs is developed.

Consider the Fourier transform of output $x_p(t)$:

$$\hat{X}_p(j\omega) = \int_0^\infty x_p(\tau) e^{-j\omega\tau} d\tau \tag{17}$$

From a numerical perspective, Eq. 17 should be considered as a sum of three components (Mopsik, 1985)

$$\begin{aligned}\hat{X}_p(j\omega) &= I_1 + I_2 + I_3 \\ &= \int_0^h x_p(\tau) e^{-j\omega\tau} d\tau + \int_h^T x_p(\tau) e^{-j\omega\tau} d\tau \\ &\quad + \int_T^\infty x_p(\tau) e^{-j\omega\tau} d\tau\end{aligned} \tag{18}$$

In Eq. 18, h refers to the fixed sampling interval and T denotes the end of the finite interval over which the sampled $x_p(t)$ data are available. The second term in sum Eq. 18 is the only component of the indefinite integral that can be obtained directly. The frequency band over which the numerical approximation to Eq. 17 is valid, is therefore limited to the interval (Mopsik, 1985)

$$\frac{1}{T} < \omega < \frac{1}{h} \tag{19}$$

Restriction Eq. 19 is necessary because at high frequencies, $\omega > h^{-1}$, term I_1 is typically dominant and it is difficult to evaluate I_1 due to the oscillatory nature of the integrand (Bailey and Swarztrauber, 1994). However, for frequencies $\omega \ll h^{-1}$, the contribution of component I_1 becomes small. At the other end of the spectrum, $T^{-1} < \omega$ term I_3 can become dominant, but the value of I_3 can only be estimated since signal $x_p(t)$ is truncated at time T.

If the Fourier integral is truncated after the hydraulic system has reached steady-state, restriction $\omega < T^{-1}$ can be removed since the value of $x_p(t)$ will be constant for $t \geq T$. Therefore, term I_3 can be computed exactly, i.e. $I_3 = x_p(T) e^{-j\omega T} \big/ j\omega$. Alternatively, one can work with time derivative $\dot{x}_p(t) = \mathcal{L}^{-1}\{sX_p^a(s)\}$. In the steady-state, $\dot{x}_p(t) = 0$ for $t \geq T$ making $I_3 \equiv 0$ in Eq. 18. The required frequency response function $\hat{X}_p(j\omega)$ can then be recovered as $\hat{X}_p(j\omega) = \hat{\dot{X}}_p(j\omega) \big/ j\omega$. A similar approach can be taken to evaluate the frequency responses, $\hat{X}_v(j\omega)$, of the actuator input signal.

In light of the above discussion, an estimate of the frequency response function for signal $x_p(t)$ can evaluated by computing the truncated Fourier integral

$$\hat{X}_p(j\omega) = \int_h^T x_p(\tau) e^{-j\omega\tau} d\tau \tag{20}$$

Calculation of the transcendental integrand in Eq. 20 is carried out by first subdividing the integration interval $(0,T]$ into N panels of length h. Then, by assuming term $x_p(\tau)$ is constant over each panel and by using a Filon-like approach (Filon, 1929) along with Euler's formula, Eq. 20 is rewritten as

$$\begin{aligned}\hat{X}_p(j\omega) = &\frac{1 - \cos(\omega h) + j\sin(\omega h)}{j\omega} \\ &\times \sum_{k=0}^{N-1} x_p(kh)[\cos(\omega kh) - j\sin(\omega kh)]\end{aligned} \tag{21}$$

Note that the sum in Eq. 21 bears resemblance to the discrete Fourier transform and can be computed efficiently using the fast Fourier transform (FFT). However, Eq. 21 offers improved accuracy over the FFT since a multiplicative factor is used to correct for the error introduced by the FFT assumption that terms '$\cos(\omega h)$' and '$\sin(\omega h)$' are constant over the integration interval. The correction factors to the left of the sum in Eq. 21 are constant at each frequency, ω. Therefore, the correction terms can be applied afterwards to the results of a FFT computation with little additional overhead. Moreover, the values of the multiplicative factors only need to be calculated once for a particular vector of frequencies. This fact can be exploited to speed the analysis of families of time signals.

Equation 21 was applied to evaluate the LTIE frequency response functions for the $x_v(t) - x_p(t)$ signal pair shown in Fig. 2. A Bode plot of the identified LTIE frequency response ratio, $P_H(j\omega) = \hat{X}_p(j\omega) \big/ \hat{X}_v(j\omega)$, is shown in Fig. 8. As can be seen, the proposed numerical procedure properly identified the low frequency integration characteristic of the ram as well as the resonant mode in the high frequency range. Moreover, the LTIE frequency response ratio obtained by Fourier transformation is identical to the one identified using Golubev's method. However, an important advantage of the Fourier transformation approach is that the LTIE frequency response function can be arrived at without the need to make assumptions on the structure of the LTIE transfer function.

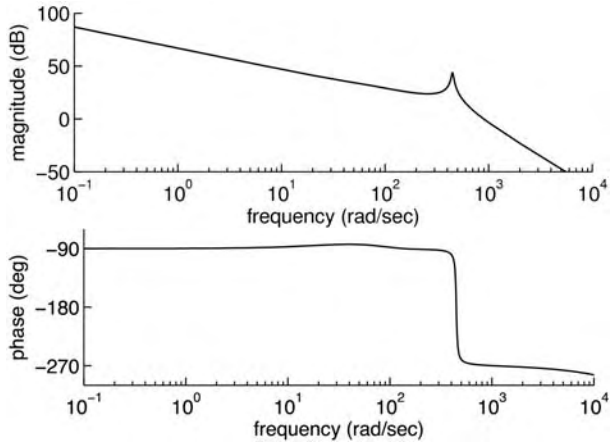

Fig. 8: *Bode plot of LTIE frequency response obtained by Fourier transformation approach*

5 Robust Control Design Example

The proposed Fourier transformation approach, described in Section 4, was applied to develop a robust two degree-of-freedom QFT position control system around an experimental electrohydraulic actuator. A photograph of the experimental setup is shown in Fig. 9. A description of the test rig has been given elsewhere (Karpenko and Sepehri, 2003) and is therefore not repeated here. The nominal parameters of the experimental actuator and the parameter uncertainties considered in the robust design are given in Table 2.

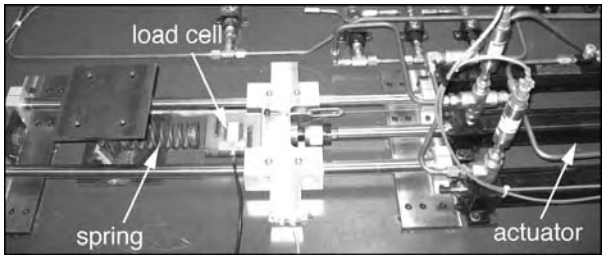

Fig. 9: *Photograph of experimental setup*

Table 2: System parameters used for controller development

fixed parameters	value		
A (mm^2)	633		
L (mm)	610		
K_v (m$^{3/2}$/kg$^{3/2}$)	0.0292		
w (mm^2/mm)	13.21		
ω_v (Hz)	150		
ζ_v	0.9		
uncertain parameters	**min**	**nominal**	**max**
P_s (MPa)	13.8	17.2	18.6
β_h (MPa)	345	689	1030
m (kg)	11	12.3	13.7
d (N/m·sec)	200	250	300
k (kN/m)	0	30	60
k_{sp} (mm/V)	0.025	0.028	0.031

Parameter uncertainty was considered in the design since variation in some hydraulic system parameters is inevitable and this can degrade the closed-loop performance. For example, the supply pressure can vary with changes in the demand for fluid and the value of the bulk modulus can fluctuate with fluid temperature (Merritt, 1967). The mass of the piston, rods, and load can be difficult to measure precisely and the value of the viscous damping coefficient often changes in different parts of the actuator stroke. Similarly, changing flow forces can impact the valve spool position gain as the servovalve ages. An uncertain load stiffness was also considered, in this paper, to account for different loading conditions under which the actuator is expected to operate. Since the QFT design technique has been well documented (Horowitz, 1993), only an outline of the approach is given here. Briefly, the design procedure involves the following steps:

5.1 Step 1 – Generating LTIE Plant Templates

The plant templates are generated from the set, $\mathcal{P} = \left\{ P_V(j\omega) \cdot \hat{X}_p(j\omega) \big/ \hat{X}_v(j\omega) \right\}$, of LTIE frequency response functions that describe the behaviour of the hydraulic actuator over the considered envelope of operation. The templates characterize, as gain and phase variation on the Nichols chart, changes in the dynamics of the hydraulic actuator that arise due to hydraulic nonlinearities and system parametric uncertainties over the set of acceptable output responses. Several templates of the experimental hydraulic actuator under consideration are shown side-by-side in Fig. 10 for selected frequencies, ω rad/sec. The template points were computed by first selecting $p_1 = 15$, $p_2 = 20$, $\omega_p = 85^2$, $\zeta_p = 1$ and $\lambda \in [14, 33]$ in Eq. 5 to generate a family of acceptable outputs for step commands of differing magnitudes. The time histories of the servo-valve spool displacements required to generate the acceptable output response set were then calculated by simulating the inverse model of the hydraulic actuator dynamics given in the Appendix. Various combinations of the uncertain hydraulic actuator parameters were considered. Finally, the magnitude and phase of the LTIE frequency response function for each input-output pair was determined at each design frequency by transforming the time-domain signals using Eq. 21.

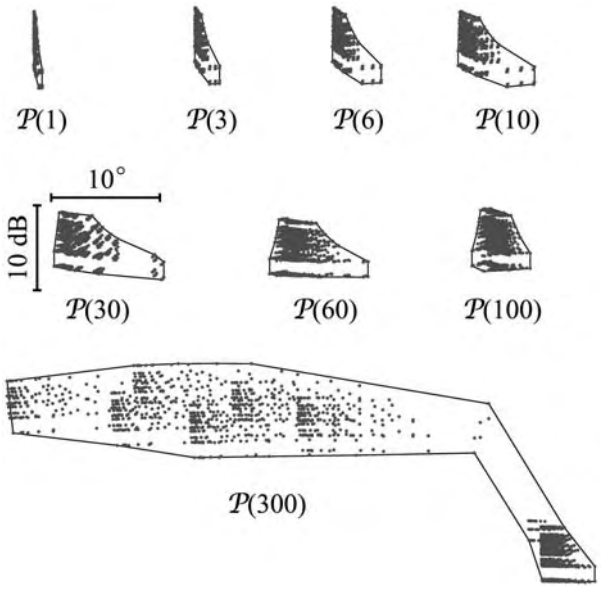

Fig. 10: *Templates of LTIE plant set, $\mathcal{P}(\omega)$, at selected frequencies, ω (rad/sec)*

5.2 Step 2 – Generating Performance Bounds and Loop Shaping

Closed-loop performance requirements on robust tracking and robust stability were translated into QFT bounds on the nominal open-loop transfer function,

$L = GP_{nom}$, where G is the transfer function of the robust controller and P_{nom} is the LTIE function of a nominal plant selected from set $\mathcal{P}$. In QFT, the entire design process is carried out in the frequency domain so it is not necessary to express P_{nom} in rational form. However, some robust synthesis techniques, for example H_∞, require a transfer function or state equation representation of the nominal LTIE model. If required, such a transfer function could be identified from the nominal LTIE frequency response using a complex curve fitting procedure such as the one described in ('t Mannetje, 1973) or (Stahl, 1984).

After selecting the nominal LTIE frequency response, the QFT bounds are derived either by moving the plant templates between the appropriate closed-loop magnitude contours (*M*-circles) on the Nichols chart or by a computer search. QFT bounds are shown in Fig. 11 at several design frequencies. The frequency response of L is then manipulated by adding controller poles and zeros until the loop shape lies in the acceptable region on the Nichols chart. The nominal loop transmission should lie above the open tracking bounds (solid lines) and outside the closed stability bounds (dashed lines) that encircle the (-180°, 0 dB) critical point. The transfer function of the robust controller is solved by evaluating ratio $G = L/P_{nom}$:

$$G(s) = \frac{2.76\times10^6(s+25)}{(s+16)(s^2+108s+120^2)} \qquad (22)$$

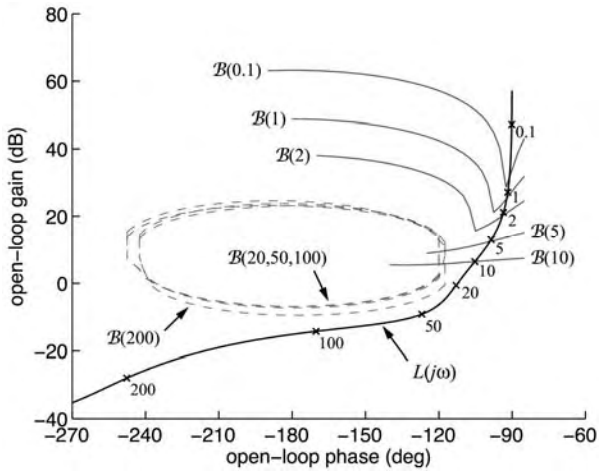

Fig. 11: *QFT bounds, $\mathcal{B}(\omega)$, and designed loop transmission, $L(j\omega)$*

5.3 Step 3 – Controller Verification

To confirm the operation of the designed robust control system, the robust controller Eq. 22 and a prefilter, designed by the QFT methodology to further shape the actuator step responses, were implemented on the hydraulic test bench. The experimental system was tested for a variety of different input commands and for different loading rates. In all the tests, good transient and steady-state performance was observed without the need to further tune the controller or prefilter. Figure 12 shows a typical closed-loop step response obtained while operating the experimental hydraulic ram against a 30 kN/m spring. Despite the large variation in the control valve drive signal, which nearly reaches the 10 V saturation level (see Fig. 12b), the actuator position response is observed to fall well within the prescribed acceptable envelope. Figure 12 thus confirms the validity of the model-based robust control system design, even for large signal operation of the electrohydraulic actuator.

5.4 Comparison with Small-Signal Approach

In order to illustrate the advantage of LTIE modelling over small-signal analysis, templates for each approach have been plotted in Fig. 13 along with the corresponding QFT bounds for ω = 1 rad/sec. For consistency, a nominal plant with $|P_{nom}(j1)| = -22.4$ dB and $\angle P_{nom}(j1) = -90.1°$, indicated by the × in Fig. 13, was selected from each of the small-signal and LTIE plant sets. Since the LTIE approach accurately models the low frequency integration characteristic of the actuator, the width of the LTIE template is small as is seen in Fig. 13. This allows it to fit alongside the *M*-circles, leading to a trough in $\mathcal{B}(1)$ that can be exploited to reduce the amount of controller gain required to realize the closed-loop specifications. On the other hand, the width of the small-signal template is much larger so the QFT bounds dictate that the template must be positioned differently in order to satisfy the *M*-circles. It can be seen from Fig. 13 that locating the small-signal template to satisfy the QFT bound requires at least 30 dB more control gain as compared to the amount needed to properly position the LTIE template. Thus, feedback is minimized by using the LTIE approach.

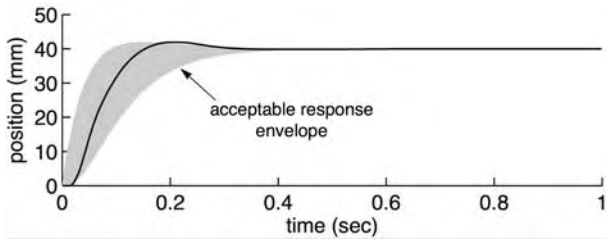

(a)

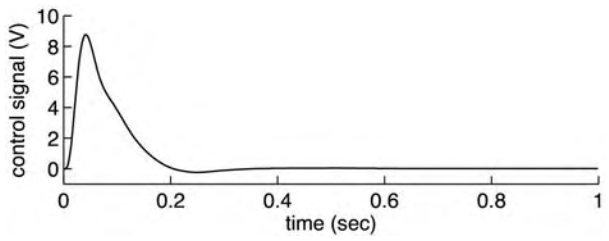

(b)

Fig. 12: *Typical experimental closed-loop position response using robust QFT controller and prefilter: (a) position; (b) control signal*

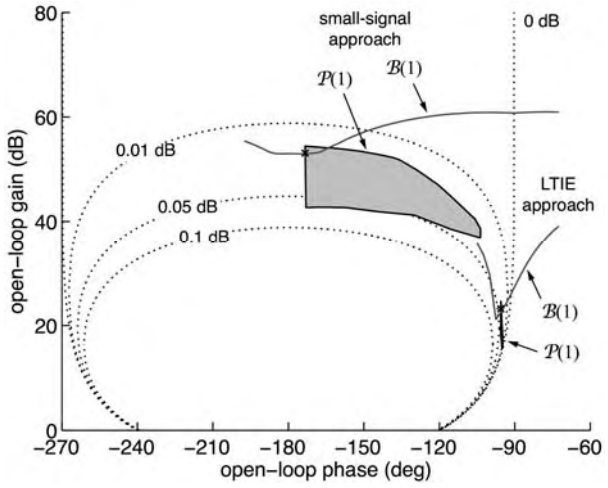

Fig. 13: *Comparison of uncertainty templates and QFT bounds obtained using small-signal and LTIE approaches for ω=1 rad/sec. Several M-circles (dotted) are shown for reference.*

6 Conclusions

This paper has investigated, from a robust control design perspective, various approaches for deriving equivalent LTI models for electrohydraulic actuators. Small-signal analysis is a common approach used to model fluid power actuators for control system synthesis. However, as demonstrated here, fixed-parameter small-signal models are generally inadequate to describe the transient response. The *LTI-equivalent* (LTIE) modelling approach, on the other hand, enables large signal responses to be accurately characterized using a fixed-gain structure, and is therefore a more appropriate choice for fluid power control system development.

A simple model-based approach for evaluating the LTIE frequency response functions was proposed in this paper. In this approach, the LTIE frequency response functions are computed directly from the actuator input-output data pairs by numerical integration of the continuous-time Fourier integral. Instead of relying on the discrete Fourier transform to perform the computation, the proposed approach employs an additional term that improves the accuracy of the quadrature. It was shown that the Fourier transformation approach is able to describe large signal effects and at the same time properly characterize the features of the hydraulic actuator frequency response that are important for robust control design. Moreover, the proposed approach does not require *a priori* knowledge about the asymptotic behaviour and structure of the LTIE transfer function, as is the case with other identification techniques such as Golubev's least-squares method.

A QFT control system design example around an experimental hydraulic ram demonstrated the applicability of the proposed numerical technique towards the development of practical fluid power control systems. This paper therefore makes further contributions to model-based hydraulic actuator control system design using a broad range of robust synthesis techniques including LQG, H_∞, μ-synthesis, and QFT.

Nomenclature

A	piston annulus area
C_d	discharge coefficient
d	viscous damping coefficient
h	sampling time
k	load stiffness
K_{1f}, K_{2f}, K_f	linearized servovalve flow gains
K_{1p}, K_{2p}, K_p	linearized flow-pressure coefficients
k_{sp}	servovalve spool position gain
K_v	servovalve flow coefficient
m	mass of piston, rods and load
o	subscript – denotes operating point
P_1, P_2	pressures in each cylinder half
P_L	load pressure
P_r	tank pressure
P_s	hydraulic supply pressure
Q_1, Q_2	control flows
Q_L	load flow
T	signal truncation time
u	servovalve control signal
V_1, V_2	cylinder volumes
v_p	piston velocity
V_T	total cylinder volume
w	orifice area gradient
x_p	piston position
x_v	servovalve spool position
β_h	effective bulk modulus of hydraulic fluid
ρ	density of hydraulic oil
ω	angular frequency
ω_v	servovalve second-order natural frequency
ζ_v	servovalve second-order damping ratio

Acknowledgments

The authors thank the Natural Sciences and Engineering Research Council of Canada (NSERC) who provided financial support for this research.

References

Bailey, D. H. and **Swarztrauber, P. N.** 1994. A fast method for the numerical evaluation of continuous Fourier and Laplace transforms. *SIAM Journal on Scientific Computing,* Vol. 15, pp. 1105-1110.

Edge, K. A. 1997. The control of fluid power systems – responding to the challenges. *Proceedings of the Institution of Mechanical Engineers Part I: Journal of Systems and Control Engineering,* Vol. 211, pp. 91-110.

Filon, L. N. G. 1929. On a quadrature formula for trigonometric integrals. *Proceedings of the Royal Society of Edinburgh,* Vol. 49, pp. 38-47.

Finney, J. M., **de Pennington, A.**, **Bloor, M. S.** and **Gill, G. S.** 1985. A pole-assignment controller for an electrohydraulic cylinder drive. *ASME Journal of Dynamic Systems, Measurement, and Control,* Vol. 107, pp. 145-150.

Golubev, B. and **Horowitz, I.** 1982. Plant rational transfer approximation from input-output data. *International Journal of Control,* Vol. 36, pp. 711-723.

Horowitz, I. 1981. Improvement in quantitative nonlinear feedback design by cancellation. *International Journal of Control,* Vol. 34, pp. 547-560.

Horowitz, I. M. 1993. *Quantitative Feedback Design Theory - QFT*, Vol. 1. QFT Publications, Boulder, CO.

Karpenko, M. and **Sepehri, N.** 2003. Robust position control of an electrohydraulic actuator with a faulty actuator piston seal. *ASME Journal of Dynamic Systems, Measurement, and Control,* Vol. 125, pp. 413-423.

Kim, M. Y. and **Lee, C.-O. 2006.** An experimental study on the optimization of controller gains for an electro-hydraulic servo system using evolution strategies. *Control Engineering Practice,* Vol. 14, pp. 137-147.

Merritt, H. E. 1967. *Hydraulic Control Systems*. Wiley, New York.

Mopsik, F. I. 1985. The transformation of time-domain relaxation data into the frequency domain. *IEEE Transactions on Electrical Insulation,* Vol. 20, pp. 957-964.

Nikiforuk, P. N. and **Westlund, D. R.** 1965. The large signal response of a loaded high-pressure hydraulic servomechanism. *Proceedings of the Institution of Mechanical Engineers,* Vol. 180, pp. 757-775.

Niksefat, N., **Sepehri, N.** and **Wu, Q.** 2007. Design and experimental evaluation of a QFT contact task controller for electro-hydraulic actuators. *International Journal of Robust and Nonlinear Control*, Vol. 17, pp. 225-250.

Piche, R., **Pohjolainen, S.** and **Virvalo, T.** 1991. Design of robust controllers for position servos using the H_∞ theory. *Proceedings of the Institution of Mechanical Engineers Part I: Journal of Systems and Control Engineering,* Vol. 205, pp. 299-306.

Plummer, A. R. and **Vaughan, N. D.** (1996) Robust adaptive control for hydraulic servosystems. *ASME Journal of Dynamic Systems, Measurement, and Control,* Vol. 118, pp. 237-244.

Sekhavat, P., **Wu, Q.**, **Wu** and **Sepehri, N.** 2005. Impact control in hydraulic actuators. *ASME Journal of Dynamic Systems, Measurement, and Control,* Vol. 127, pp. 197-205.

Stahl, H. 1984. Transfer function synthesis using frequency response data. *International Journal of Control,* Vol. 39, pp. 541-550.

't Mannetje, J. J. 1973. Transfer-function identification using a complex curve-fitting technique. *Journal of Mechanical Engineering Science,* Vol. 15, pp. 339-345.

Whitfield, A. H. and **Messali, N.** 1987. Integral-equation approach to system identification. *International Journal of Control,* Vol. 45, pp. 1431-1445.

Wu, D., **Burton, R.**, **Schoenau, G.** and **Bitner, D.** 2002. Establishing operating points for a linearized model of a load sensing system. *International Journal of Fluid Power,* Vol. 3, pp. 47-54.

Appendix – Inverse Hydraulic Actuator Model

Consider the nonlinear description of the hydraulic actuator dynamics given by Eq. 1. The time histories of acceptable $x_v(t)$ are computed numerically from acceptable position trajectories, $x_p(t)$, using the approach described previously in Niksefat and Sepehri (2007).

Differentiating and manipulating Eq. (1b), which describes the dynamics of the piston, leads to the following relation:

$$A(\dot{P}_1 - \dot{P}_2) = m\dddot{x}_p + d\ddot{x}_p + k\dot{x}_p \tag{23}$$

Using Eq. 1c and Eq. 1d along with Eq. 2 and Eq. 23, a system of linear equations $\mathbf{A}\boldsymbol{x} = \boldsymbol{b}$, with solution vector $\boldsymbol{x} = [\dot{P}_1, \dot{P}_2, x_v]^T$, can be formed where

$$\mathbf{A} = \begin{bmatrix} A & -A & 0 \\ 1 & 0 & \dfrac{-K_v w \beta_h}{V_1}\sqrt{\dfrac{P_s - P_r}{2} + \dfrac{x_v}{|x_v|}\left(\dfrac{P_s + P_r}{2} - P_1\right)} \\ 0 & 1 & \dfrac{K_v w \beta_h}{V_2}\sqrt{\dfrac{P_s - P_r}{2} + \dfrac{x_v}{|x_v|}\left(P_2 - \dfrac{P_s + P_r}{2}\right)} \end{bmatrix} \tag{24}$$

and

$$\boldsymbol{b} = \left[m\ddot{x}_\mathrm{p} + d\dot{x}_\mathrm{p} + kx_\mathrm{p},\quad -\frac{\beta_\mathrm{h} A\dot{x}_\mathrm{p}}{V_1},\quad \frac{\beta_\mathrm{h} A\dot{x}_\mathrm{p}}{V_2} \right]^\mathrm{T} \qquad (25)$$

Using the time derivatives of $x_\mathrm{p}(t)$, the linear system formed by Eq. 24 and Eq. 25 is solved for the corresponding values of variables x_v, $\dot{P}_1$, and $\dot{P}_2$. To propagate the inverse model forward in time, the previously solved pressure derivatives, $\dot{P}_1(t_\mathrm{i})$ and $\dot{P}_2(t_\mathrm{i})$, are integrated using Euler's forward method. The results of the numerical integration are the values $P_1(t_{\mathrm{i}+1})$ and $P_2(t_{\mathrm{i}+1})$, which are used to solve the system of equations at the next time step.

Mark Karpenko
is currently completing his Ph.D. degree in Mechanical Engineering at the University of Manitoba, and holds B.Sc. and M.Sc. degrees from the same University. His research interests include robust control of fluid power systems and, in particular, fault tolerant control. He has published several papers on QFT control system design for hydraulic and pneumatic servos.

Nariman Sepehri
is a professor with the Department of Mechanical and Manufacturing Engineering, at the University of Manitoba. He received M.Sc. and Ph.D. both from the University of British Columbia, Canada. His areas of interest include telerobotics applied to hydraulic manipulators and fluid power fault tolerant control and diagnosis systems.